r-reviewed version available at The International Journal of Advanced Manufacturing Technology 2020, 108, 1725-1735; doi:10.1007/s00170-020-055

Article

A Comparative Study of Tensile Properties between Fused Filament Fabricated and Injection-Molded Wood-PLA Composite Parts

M. Damous Zandi[a], Ramon Jerez-Mesa[b], Jordi Llumà[c], Jordi Jorba-Peiro[c] and J. Antonio Travieso-Rodriguez[a]

[a] Universitat Politècnica de Catalunya, Escola d'Enginyeria de Barcelona Est, Mechanical Engineering Department, Avinguda d'Eduard Maristany, 10-14, 08019 Barcelona, Spain

[b] Universitat de Vic – Universitat Central de Catalunya, Faculty of Sciences and Technology. Engineering Department. C. Laura, 13. 08500 Vic, Spain

[c] Universitat Politècnica de Catalunya, Escola d'Enginyeria de Barcelona Est, Materials Science and Metallurgical Engineering Department, Avinguda d'Eduard Maristany, 10-14, 08019 Barcelona, Spain

Abstract: The present study evaluates the manufacturing parameters effects on the tensile properties of material composed by polylactic acid (PLA) with wood fibers known as Timberfill. The specimens were built through fused filament fabrication (FFF). The influence of four printing parameters (Layer height, Fill density, Printing velocity, and Orientation) are considered through a L_{27} Taguchi orthogonal array in order to reduce experimental runs. Tensile test is applied to obtain the response variable used as output results to perform the ANOVA calculations. Fill density is the most influential parameter on the tensile strength, followed by building orientation and layer height, whereas the printing velocity shows no significant influence. The optimal set of parameters and levels is found, being 75% fill density, 0°Z-axis orientation, 0.4 mm layer height, and 40 mm/s velocity as the best combination. Applying this combination showed 9.37 MPa in maximum tension. Lastly, five solid Timberfill specimens manufactured via injection molding technology were also tested and the results compared to the printed samples. The values of the elastic modulus, elastic limit, and maximum tension of the injected samples were almost twofold of those were obtained for the FFF samples, but the maximum elongation of injected specimens was fell sharply.

Keywords: additive manufacturing; 3D printing; fused filament fabrication; Young's module; tensile strength; Timberfill; PLA

1. Introduction

Additive manufacturing (AM) has already gained traction in the aerospace and biomedical industries and is now being explored as a viable manufacturing method in the construction sector. Fused Filament Fabrication (FFF) or 3D printing is one of the most common AM technique to fabricate complex three-dimensional components to a near-net shape. The mechanical performance of FFF 3D printed parts depend on several manufacturing process and design parameters. Examples of manufacturing process parameters include machine tolerances, feedstock material, filament diameter, nozzle diameter, nozzle temperature, bed temperature, cooling rate (i.e. fan speed), and printing velocity [1,2]. On the other hand, there are examples of design parameters include building orientation, raster angle, layer thickness, and infill percentage [3,4].

Numerous studies have investigated the effects of aforementioned parameters on the tensile strength and the other mechanical properties of applicable materials. Es-Said, O.S. et al. [5] have examined the effect of layer orientation on the mechanical properties of rapid prototype ABS P400

samples by performing tensile, three-point bending, and impact tests. The tensile data of the ABS samples with different orientations indicate that the ultimate and yield strengths were the highest in the orientation where layers were deposited along the length of the sample (0° in X-axis), followed by those where the samples are built at 45°, -45° and 90° in descending order. In [6] influence of five important process parameters such as layer thickness, orientation, raster angle, raster width and air gap on three responses such as tensile, flexural and impact strength of test specimen are considered. In this study the desirability function concept have been used to determine optimal factor levels for improving tensile, flexural and impact strength independently and all three strengths simultaneously. In another study Fernandez-Vicente, M. et al. [7] the influence of two controllable variables, such as pattern and density of the infill of samples produced using an open-source 3D printer on the tensile mechanical behavior has been evaluated. The results obtained show that the influence of the different printing patterns causes a variation of less than 5% in maximum tensile strength, although the behavior is similar. The change in infill density determines mainly the tensile strength. The combination of a rectilinear pattern with a 100% infill shows the higher tensile strength, with a value of 36.4 MPa, with a difference of less than 1% from raw ABS material. A study made by John J. Laureto et al. [8] characterized the mechanical property variations of ultimate tensile strength (UTS) and yield strength of FFF printed components of ASTM D638-14 Type I and Type IV tensile bar specimens, and multiple parameter types were evaluated for PLA material. The results show that the influence of different printing patterns varies the maximum tensile strength less than 5%. The combination of a rectilinear pattern in a 100% infill shows the higher tensile strength, with a value of 36.4 MPa, with a difference of less than 1% from raw ABS material.

Cwikła, G. et al. [9] have concluded the infill pattern, fill density, shell thickness and printing temperature influence on the selected mechanical properties of the standardized samples, printed with low-cost standard materials (ABS), using a low cost 3D printer. The results show that, where the objective is to have both, a lightweight and durable element, the best set of parameters is the use of a honeycomb pattern with fill density of about 40-50%, and a shell thickness of 2-3 layers/lines. If the maximum strength is the priority, shell thickness should be increased. The use of an infill pattern other than the honeycomb can accelerate the time of printing at the expense of its strength. Tensile test has also shown that the extrusion multiplier parameter should not be set less than 0.9, because strength of the sample decreases disproportionately to filament savings. Marat-Mendes, R. et al. [10] have studied the influence of Fused Filament Fabrication processing parameters such as extrusion temperature and raster angle upon mechanical properties and microstructural features of processed PLA parts. In this research the fill density, layer thickness and printing velocity were kept constant at 60 %, 0.2 mm and 40 mm/s, respectively. The results indicates that mechanical performance is higher when material is stored under controlled atmosphere before use, and when material deposition direction is aligned with applied load. Increasing the extrusion temperature also increases performance, by increasing deformation ability of PLA molecules. This study focuses on the influence of nozzle temperature and infill line orientations for parts made with short carbon fiber (CF)-reinforced PLA. Results have shown the influence of nozzle temperature on the mechanical properties, with an optimum temperature maximizing the tensile properties. Infill orientations also play a significant role in achieving good mechanical properties, with the proper combination of orientation enabling the tailoring of properties along a specific axis, according to El Magri, A. et al. [11].

Also researchers observed behavior of parts fabricated with different manufacturing technologies [12-14], and different treatments [15-18] to achieve higher resistances of mechanical properties. The authors in [19] have presented the application of agro-waste materials (i.e., corn stalk, reed stalk, and oilseed stalk) in order to evaluate and compare their suitability as reinforcement for thermoplastics as an alternative to wood fibers. Overall trend shows that with addition of agro-waste materials, tensile and flexural properties of the composites are significantly enhanced. The tensile and flexural properties of the composite significantly decreased with increasing $CaCO_3$ content, due to the reduction of interface bond between the fiber and matrix. Tufan, M. et al. in another study have investigated the effect of heat-treated wood content on the water absorption, mechanical, and thermal

properties of wood plastic composites (WPC). The mechanical property values of the WPC specimens decreased with increasing amounts of the heat-treated flour, except for the tensile module [20].

To reduce the consumption of petroleum-based resources and thereby enhance the eco-friendliness of the material, it could be interesting to replace parts of ABS with other materials such as PLA or other composites and renewable materials for same purposes. To this extend other researches have compared mechanical characterizations of different materials. The results of study quantifying the basic tensile strength and elastic modulus of printed components using realistic environmental conditions for standard users of a selection of open-source 3D printers from [21] shows that parts printed from tuned, low-cost, open-source RepRap 3D printers can be considered as mechanically functional in tensile applications.

However, it is essential characterize and understand the performance of FFF-processed Timberfill parts. That is why the aim of the current investigation is to examine the effects of printing parameters of innovative Timberfill specimens on the tensile mechanical properties. To avoid manufacture a big number of specimens an experimental design of Taguchi L_{27} orthogonal array was applied that refers to how participants are allocated to the different conditions. Then to evaluate the achieved characteristics of printed Timberfill samples, a comparison was made between injection-molded and printed sample applying the same procedure. This provides a point of comparison to assess the properties achieved by the printed specimens. It is also the main novelty of this paper, since there are no reported studies in the literature that discuss the differences between the properties of 3D printed parts and those obtained by other classic manufacturing technology.

2. Materials and methods

Timberfill "Rosewood" filament of 1.75 mm diameter developed and manufactured by company Filamentum Ltd. located in the Czech Republic was used to manufacture the specimens for this study. Basically, Timberfill was developed with a purely aesthetic purpose that of imitating objects with a wood aspect. To achieve that objective, the company developed a composition of biodegradable PLA polymer combined with wood fibers in a 5%-10% ratio. Therefore, Timberfill can be proven to be a feasible material for some practical purposes in low-scale manufacturing environments.

Timberfill is a relatively new PLA-wood composite material that exhibits similar mechanical features as ABS or PLA. Models printed with this material have a genuine appearance of wood. It is provided as a commodity material, with the purpose of becoming a commonly used material in FFF machines for various applications.

2.1. Tensile testing and specimens

The tensile specimens in this work were manufactured according to ASTM D-638 standard test method for tension of plastics and composites utilizing dog-bone shape as shown in Fig.1, with 7mm thickness. In this study, Elastic modulus (Young's modulus), Elastic limit (Yield strength), Tensile strength, and maximum Elongation to break measurements are measured to characterize the mechanical behavior of Timberfill pieces submitted to tensile loads.

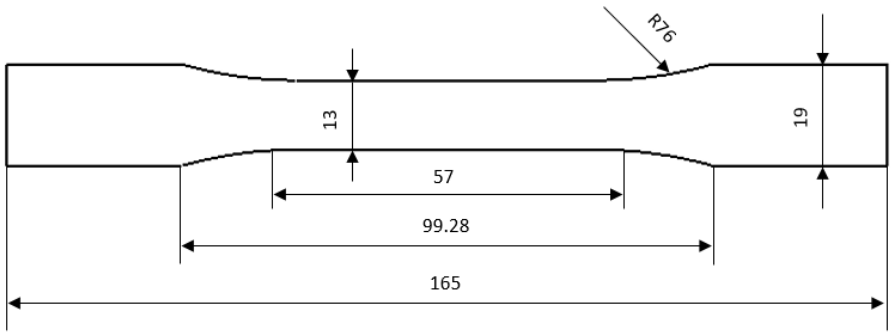

Figure 1: Geometrical drawing of specimens for tensile test

2.2. Taguchi *experimental design*

To carry out the study an experimental design (DOE) has been applied based on Taguchi method which is a robust optimization technique to make experimental to predict responses and optimize the FFF process conditions in accuracy level [22]. The factors and levels shown in Table 1, have been chosen taking into account their high effectiveness on mechanical properties rely on previous researches [23], printer configurations, and material manufacturer recommendations. Due to Timberfill is a composition of PLA polymer with wood fibers, the manufacturer recommended to extrude it with minimum 5 mm nozzle diameter. Finally it has been decided to select layer height, fill density, printing velocity, and building orientation (Table 1).

Table 1: Factors and levels used for the DOE

Parameters		Level		
		1	2	3
Layer height	**(mm)**	0.2	0.3	0.4
Fill density	**(%)**	25	50	75
Velocity	**(mm/s)**	30	35	40
Orientation		X-axis	45º X-axis	Z-axis

To clarify the selected parameters, figure 2 shows a definition of them to how determined in the slicer software used for print the samples. The cut section of the samples which indicates the different orientation with 50% density of grid infill patter (Fig. 2A). In figure 2B, the height of the Layers depositing on top the previous one is shown.

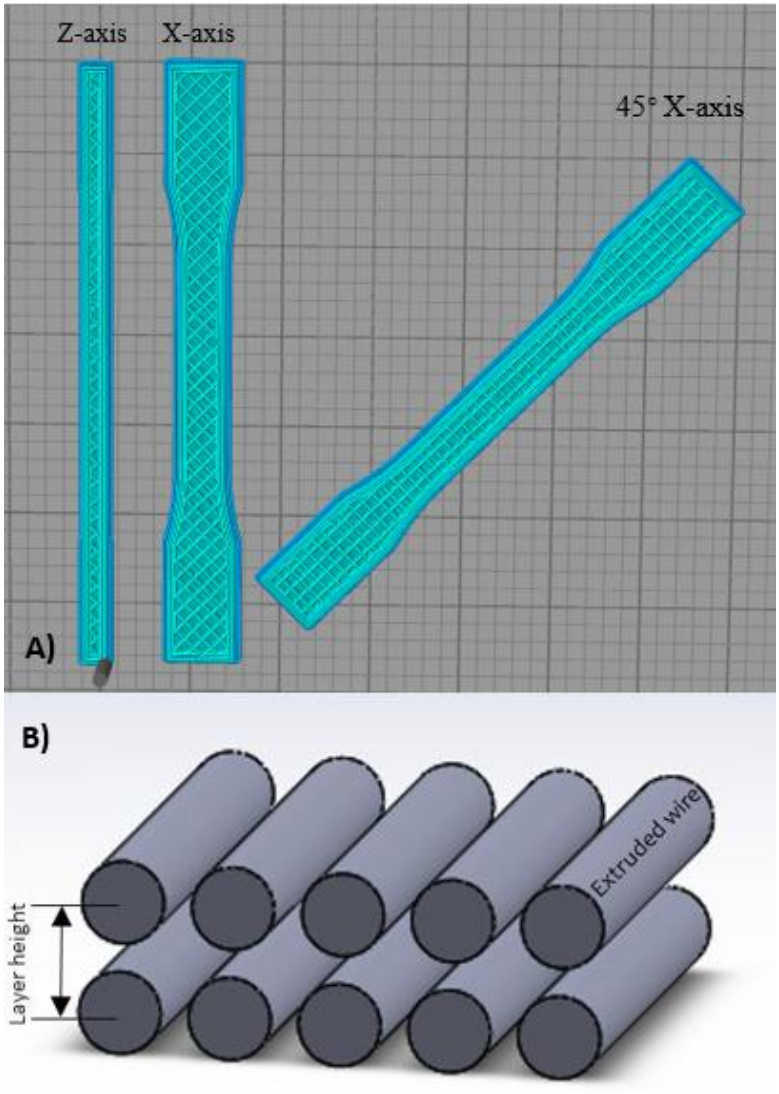

Figure 2: A) Different orientation and cut section of the samples with 50% density in grid infill pattern. B) The height of the extruded layers

To analyze the influence of the selected factors and levels a L_{27} Taguchi orthogonal array has been applied using Minitab 18 software for statistical calculations (Table 2).

Table 2: L27 Taguchi orthogonal array of DOE

Runs	Layer height (mm)	Fill density (%)	Velocity (mm/s)	Orientation
1	0.2	25	30	X-axis
2	0.2	25	35	45º X-axis
3	0.2	25	40	Z-axis
4	0.2	50	30	45º X-axis
5	0.2	50	35	Z-axis
6	0.2	50	40	X-axis

7	0.2	75	30	Z-axis
8	0.2	75	35	X-axis
9	0.2	75	40	45º X-axis
10	0.3	25	30	45º X-axis
11	0.3	25	35	Z-axis
12	0.3	25	40	X-axis
13	0.3	50	30	Z-axis
14	0.3	50	35	X-axis
15	0.3	50	40	45º X-axis
16	0.3	75	30	X-axis
17	0.3	75	35	45º X-axis
18	0.3	75	40	Z-axis
19	0.4	25	30	Z-axis
20	0.4	25	35	X-axis
21	0.4	25	40	45º X-axis
22	0.4	50	30	X-axis
23	0.4	50	35	45º X-axis
24	0.4	50	40	Z-axis
25	0.4	75	30	45º X-axis
26	0.4	75	35	Z-axis
27	0.4	75	40	X-axis

It should be mentioned that for each manufacturing parameter set or run included in the array, 5 specimens were manufactured and tested, to guarantee the repeatability of the results. Therefore, the rest of the parameters that are not object of study have been kept constant among all specimens (Table 3).

Table 3: Main constant printing parameters used in the experiments.

Nozzle diameter	Raster angle	Nozzle temperature	Infill pattern	Skirt layer
0.5 mm	45º	180ºC	Grid	2 layers

2.3. Specimens manufacture

According to the above-mentioned test method, the sample was designed by the Catia V5 software with the actual shape and dimensions and has been exported to an STL format, so that it can be read and interpreted by the printing parameterization software. In this project, the Repetier-Host

software has been used which the G-Code is obtained to be able to print. All of the specimens were printed using Prusa i3 printer.

Five specimens were also manufactured through the injection process. The same raw material used for the printed specimens was used for this. In this way the results obtained can be comparable. These specimens were manufactured with the following condition defined in table 4.

Table 4: Manufacturing conditions of the injection-molding samples

	Injection property				
Quantity	Injection pressure	Temperature	Injection time	Maintaining time	Cooling duration
	35-65 bars	200°C	76 s	30 s	10 s

2.4. Experimental setup

Once all the samples were manufactured, they have been measured to achieve the average area by calculating from the width and thickness of four different point of samples using digital micrometer.

The universal Microtest EM2/20 machine has been used for these tensile tests equipped with a 25 kN load cell at a 1 mm/min displacement rate, 50 mm extensometer, a Spider and Microtest data acquisition system, two S1 pneumatic jaws, and the Microtest SCM3000-Catman 4.5 control software. In the other side, this setup consist of a set of a High Definition (HD) camera that records the test video at 60 Hz sampling frequency, which is also connected to the spider data logger. The camera has equipped with a switch-controlled flash to illuminate the test area and to synchronize the data (Fig. 3).

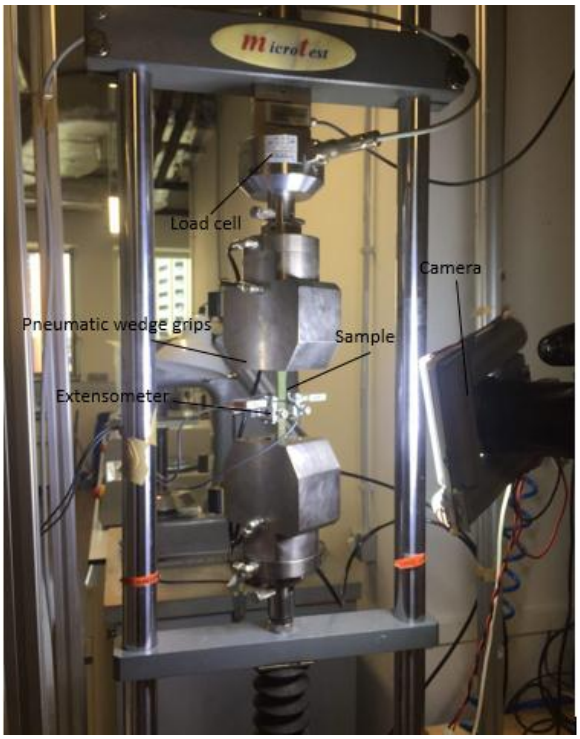

Figure 3: Universal testing machine with camera and load equipment assembly

Once all the setup is equipped and adjusted, the tests are carried out for all of the 135 FFF specimens and the 5 injected samples.

2.5. Analyzing process

After each test has been completed, two different files are achieved from the data logger. First, a file that includes the force collected from the load cell and displacement of the extensometers, as well as the recorded voltage versus time. Second, the video recorded by the camera that provided graphical information to compute the strain of the specimen at every stage of the test.

To obtain the defined mechanical properties such as Young's modulus (E), yield strength ($Rp_{0.2}$), maximum strength (σ_{max}), and maximum deformation (ε), Matlab R2018b software is used to analyze the data. To perform this analysis, several steps have been followed. First of all, the HD video was processed to obtain each photo frame during the test. In the second step, the photo frames and the recorded data are synchronized by means of a Matlab script. Next, a rectangular grid pattern is generated in the initial frame of the test sample that shown with red crosses (Fig. 4. A). This gridding recognizes the displacement on the section of samples which the deflection occurs (Fig. 4. B). During the next step, the marked pixels are tracked and deflection is computed consequently based on the differences between the initial and final position. By finishing this step, two scroll files have been generated which can be used for the deflection script to transfer the values of the points into real deformations. After using the deflection obtained in this step, the process continues to calculate the deformation and create the stress-strain curve.

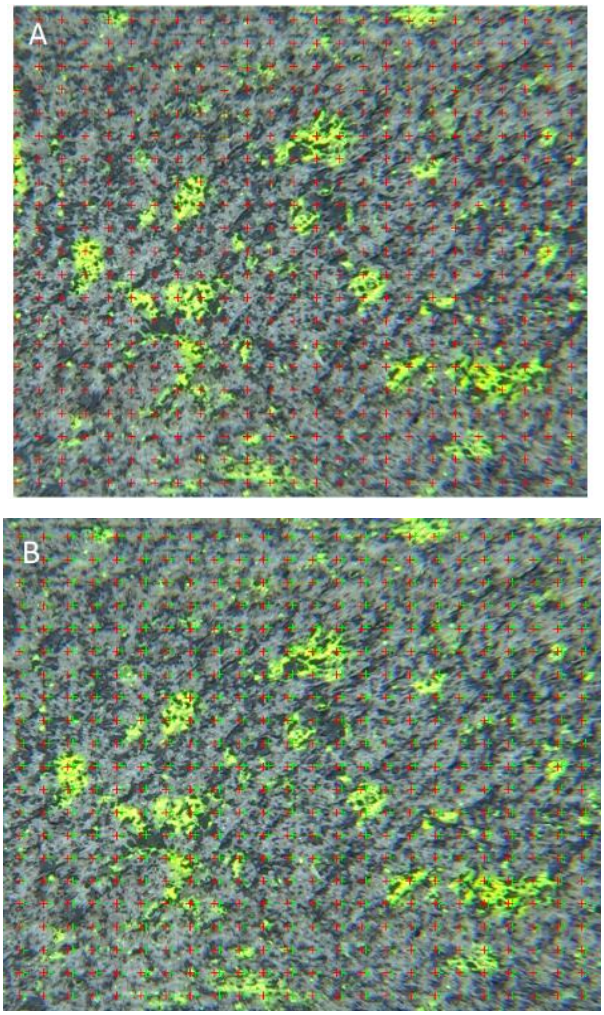

Figure 4: A) Rectangular grid generated on the test section of sample tracking with red points. B) Initial points and displaced points

3. Results analysis

Table 5 includes the average results of the five repetitions for each manufacturing configuration.

208 *Table 5: Results obtained for experimental runs. E: Young's modulus, $Rp_{0,2}$: yield strength, σ_{max}: maximum strength, ε:*
209 *maximum deformation, Std: standard deviation for each property.*

#	E (GPa)	Std	$Rp_{0.2}$ (MPa)	Std	σ_{max} (MPa)	Std	ε	Std
1	0.65	0.06	4.50	0.48	4.93	0.60	1.34	0.25
2	0.60	0.03	4.21	0.20	4.84	0.22	2.03	0.21
3	0.71	0.02	4.97	0.24	5.16	0.40	1.06	0.17
4	0.64	0.00	4.98	0.14	5.73	0.29	2.04	0.50
5	0.80	0.03	5.54	0.06	5.97	0.16	1.42	0.27
6	0.72	0.02	4.83	0.17	5.39	0.22	1.90	0.19
7	1.06	0.07	7.07	0.15	7.81	0.13	2.01	0.10
8	0.93	0.06	6.03	0.31	6.73	0.31	1.77	0.15
9	0.91	0.03	6.84	0.41	8.17	0.52	2.63	0.35
10	0.58	0.02	4.31	0.26	5.05	0.26	2.23	0.45
11	0.74	0.05	5.61	0.70	6.17	0.55	1.78	0.37
12	0.68	0.01	4.78	0.13	5.26	0.12	1.65	0.11
13	0.98	0.06	7.02	0.24	7.37	0.19	1.28	0.09
14	0.79	0.02	5.74	0.18	6.36	0.19	2.34	0.15
15	0.69	0.05	5.43	0.48	6.43	0.57	3.03	0.60
16	0.81	0.02	5.67	0.11	6.34	0.12	2.36	0.25
17	0.81	0.03	6.19	0.20	7.63	0.25	3.56	0.50
18	1.21	0.05	8.95	0.30	9.37	0.27	1.42	0.12
19	0.72	0.00	5.25	0.10	5.67	0.17	1.41	0.15
20	0.77	0.02	5.82	0.23	6.35	0.16	1.75	0.29
21	0.65	0.02	4.84	0.19	5.58	0.26	2.69	0.37
22	0.87	0.02	6.61	0.14	7.22	0.18	1.95	0.25
23	0.70	0.01	5.68	0.19	6.55	0.25	2.35	0.29
24	1.13	0.20	7.61	0.48	8.15	0.37	1.13	0.10
25	0.88	0.04	6.71	0.18	7.94	0.31	2.35	0.43
26	1.20	0.07	8.90	0.32	9.11	0.42	1.27	0.23
27	1.06	0.03	7.82	0.09	8.55	0.04	2.42	0.50

210 ### 3.1. *Analysis of variance*

211 Once the results were obtained, the statistical calculation through analysis of variance (ANOVA)
212 was performed on the dataset included in the Taguchi experimental array, for each parameter that
213 describe the mechanical behavior of the evaluated specimens by the Minitab 18 software. To validate
214 the statistical significance of the parameters included in the model on each of the responses, the p-
215 value associated to the ANOVA, was compared to a significance level of 5%. In addition, the
216 interactions between the different parameters were analyzed which leads to the conclusion that if
217 there is significant interaction among the pairs of selected values or not, since the p-values of each
218 pairs should be less than 0.05.

219 #### *3.1.1. Young's modulus*

220 In this case, it can be concluded that the most significant parameters, due to their p-values, are
221 the fill density and orientation as shown in Fig. 5. This graph evidences that the fill density results
222 have a direct relation with the Young's modulus that means higher values of density results in a
223 higher elastic module. As it can be seen from the figure, the samples built in Z-axis orientation have
224 shown higher elastic modulus. Based on the obtained p-values, layer height can be taken into account

because the value is not so much bigger than 0.05, but printing velocity does not show a significant effect on the Young's modulus.

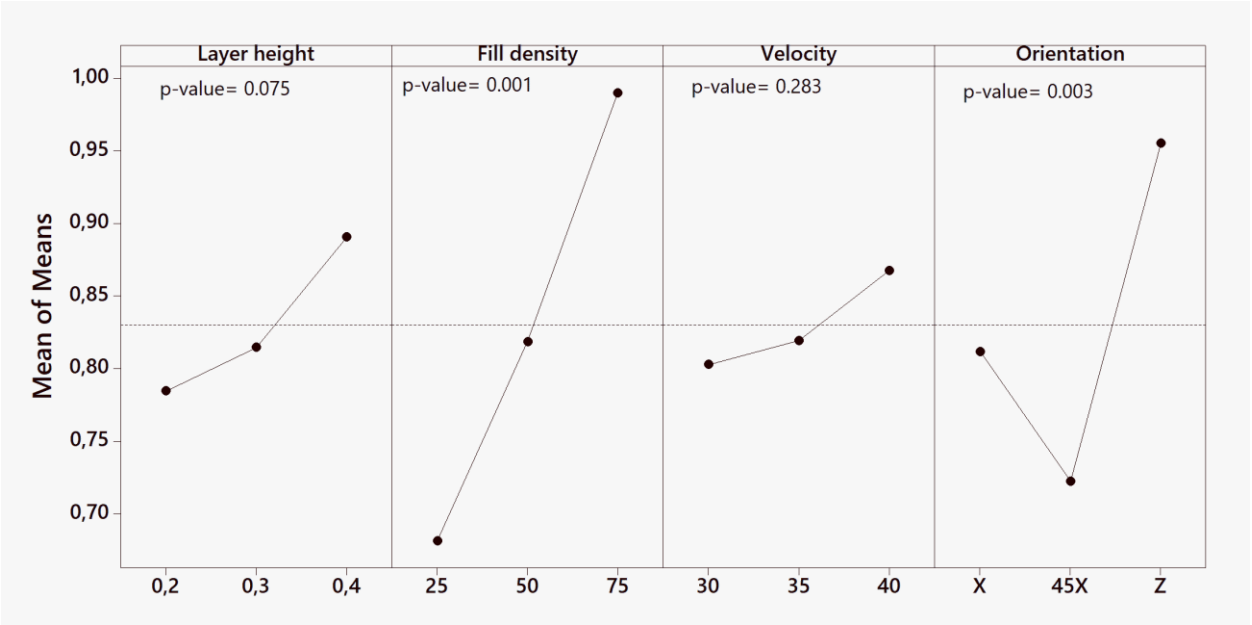

Figure 5: Main effect for means calculated through ANOVA. Response variable: Young's module

In this case obtained p-values of parameters interactions were more than 0.05, it means that the selected parameters in this study are independent of each other, at least in the analyzed value ranges for Young's modulus.

3.1.2. Yield Strength

It is necessary to analyze the effects of the variation of the different factors on the yield strength, which is indicated in graph of main effects for the averages (Fig. 6). The most significant parameters on the yield strength according to the p-values are fill density, followed by orientation and layer height. To achieve the bigger yield strength, the bigger values of layer height and fill density and Z-axis orientation should be selected.

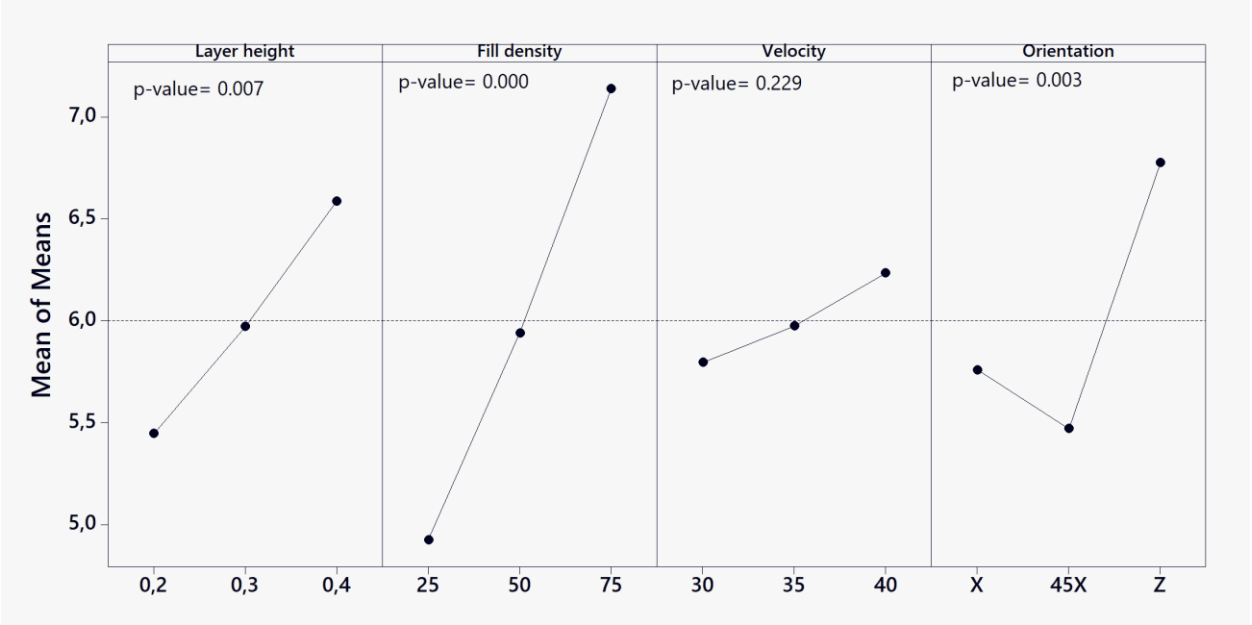

Figure 6: Main effect for mean effects calculated through ANOVA. Response variable: yield strength

Similar to the interaction between parameters on Young's modulus, the p-value does not show significant on yield strength. It means, there is no influential interaction between parameters.

3.1.3. Maximum strength

Regarding the obtained p-values from the factors on maximum strength as shown in Fig. 7, the most significant parameters are fill density, layer height, and orientation in descending order. Printing velocity has not as significant effect on this property.

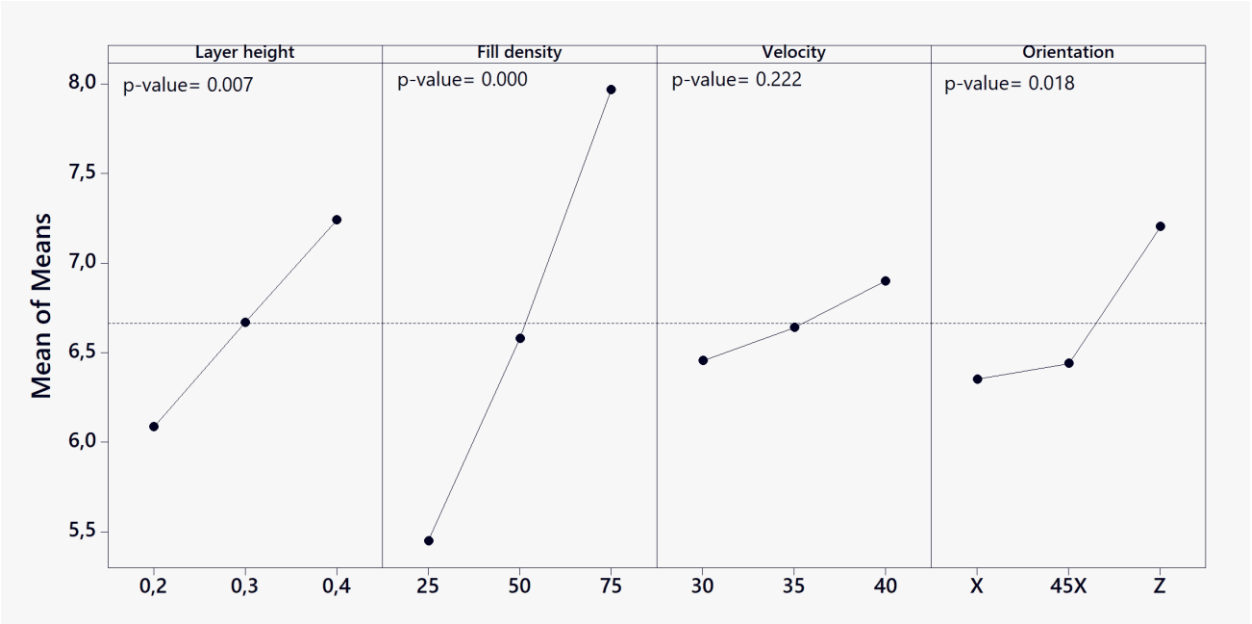

Figure 7: Main effect for mean effects calculated through ANOVA. Response variable: maximum strength

The obtained p-values of interaction are higher than 0.05, therefore the interaction between parameters should not be taken into account as a significant, like in the previous properties analyzed.

3.1.4. Maximum defomation

In case of maximum deformation, the fill density, layer height and velocity are not an influential parameters whereas building orientation has shown remarkable effect on the maximum deformation according to the p-values. The higher maximum deformations are obtained from those specimens printed at 45° on X-axis orientation, shown in Fig. 8. Also the obtained p-values of interaction for this response are higher than 0.05, therefore the interaction between parameters should not be taken into account as a significant.

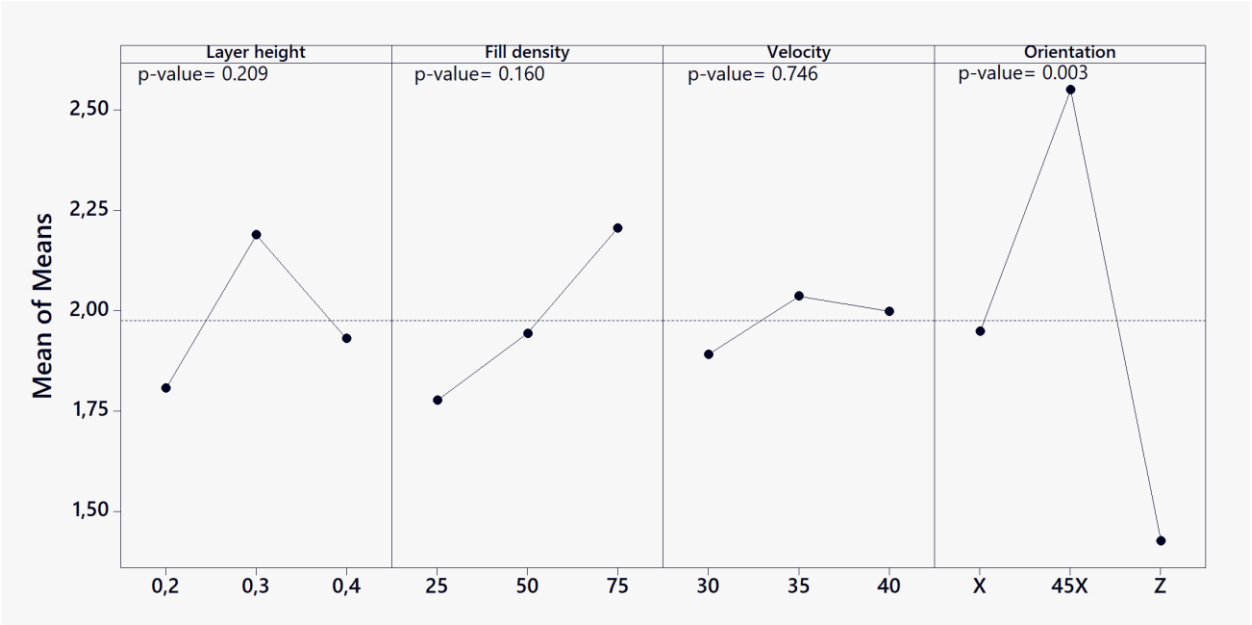

Figure 8: Main effect for mean effects calculated through ANOVA. Response variable: maximum deformation

3.2. *Results discussion*

An overview of the results is summarized in table 6. Based on the p-values the most influential parameters and the levels on the responses are indicated in the relevant cells.

Table 6: Summary of significances on responses

Response		Influential Parameter
Young's Modulus (E)	Elastic properties	Fill Density: 75% Orientation: Z-axis
Yield Strength ($Rp_{0,2}$)		Fill Density: 75% Orientation: Z-axis Layer height: 0.4
Maximum Strength (σ_{max})	Plastic properties	Fill Density: 75% Layer height: 0.4
Maximum Deformation (ε)		Orientation: 45°X-axis

These results evidence that each of the analyzed parameters is related to a different stress-strain functional regime of the FFF Timberfill material. Since the deposited layers direction in building Z-axis orientation is aligned to the test axis, it causes the material to endure the stress and the effectiveness of this parameter in elastic regime. According to the literature [24], specimens built in the X-axis direction (the long axis of the specimens is directed towards the tray`s X direction, 0o relative to the X-Y plane) exhibited higher strength (maximum load and stress) values, compared to the strength measured on three point bending specimens built in the Z direction.

It is clear that the solidity (infill) percentage of the samples can increase the mechanical properties' values, so this parameters could vary based on the desired applicability. Also it can be seen from the results of [23], the nozzle diameter and fill density are the most influence parameters on the ultimate tensile strength, yield strength, and elastic modulus of produced ABS parts.

The final result for the optimized set of parameters are shown in table 7. It is worth mentioning that, as the printing velocity is not influential in any case, the highest value has been taken for the sake of productivity.

Table 7: Optimized set of parameters and their levels

Factor	level
Layer height (mm)	0.4
Density (%)	75
Printing velocity (mm/s)	40
Orientation	Z-axis

3.3. *Comparison between FFF and Injected results*

Engineering stress-strain curves achieved from printed and injected samples are shown in Fig. 9. The average of achieved values of Young's modulus, yield strength, maximum strength, and maximum deformation from the FFF manufactured samples are almost ½ of which obtained from the injected samples, while the maximum deformation average of injected samples is lower than FFF samples observably (Table. 8), meaning the injection process enhances the overall behavior of the material.

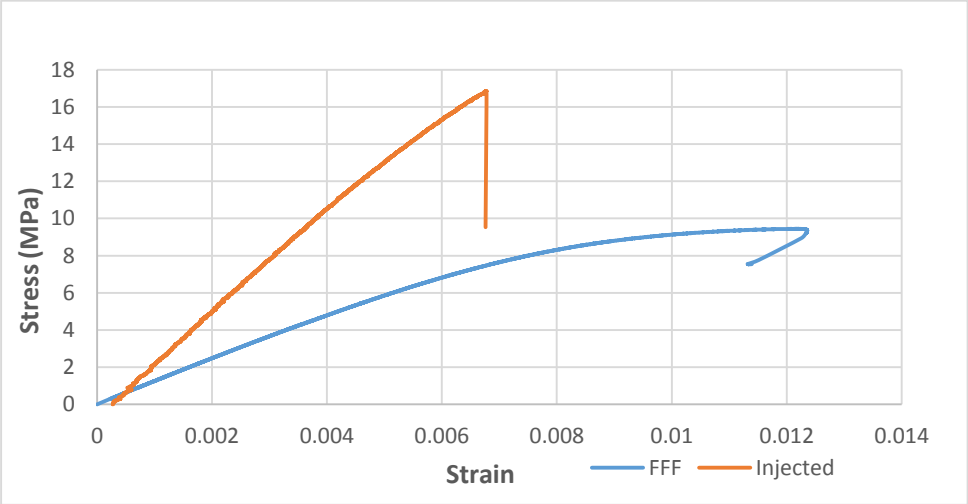

Figure 9: Strain-stress curve of FFF and injected Timberfill

Table 8: Comparison of maximum values of all mechanical properties achieved for injected and FFF results

Maximum values		
Timberfill	**Printed**	**Injected**
Young's Modulus (GPa)	1.21	2.81
Yield Strength (MPa)	8.95	16.47
Maximum Strength (MPa)	9.37	16.95
Maximum Deformation (%)	3.56	0.51

Since, the tensile stresses are produced across the whole cross section; the injected specimen demonstrated higher strength to the tension than printed specimens when they are submitted to tensile test. The printed sample meets smaller mean failure which agrees to the solidity percentage of the samples. In contrary, the higher the maximum deformation of printed sample can be due to the disengagement of the extruded wires one by one.

4. Fractography

To clarify the failure mode submitted to tensile test for both injected and printed samples, a cross-section fractographies of broken zone have taken by a Moticam 3 digital camera through a Motic SMC binocular (Fig. 10). According to the nature of the material, both different manufactured parts shown brittle behavior to which there are no sign of extending zone due to plasticity. The main reason of this phenomenon could be the poor tenacity of the wood fibers to matrix that causes an interruption to the molecular chain of the matrix.

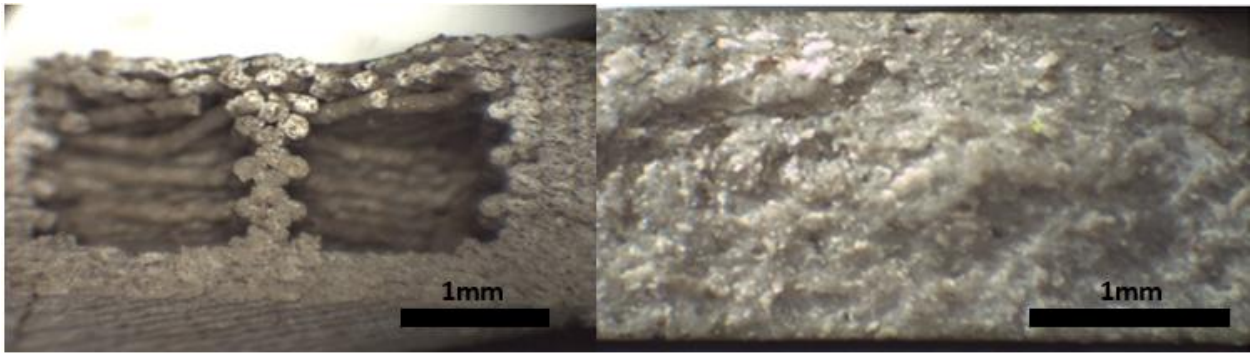

Figure 10: Fractographies of Timberfill specimens. A) 25 % infill printed. B) Injection-molded

5. Conclusions

This study shows the effects of different printing parameters on the mechanical properties of wood-reinforced PLA (Timberfill) material. The selected parameters in this work are: Layer height, fill density, printing velocity, and orientation. The mechanical properties that are object of this research are Young's modulus, Yield Strength, Maximum Strength, and Maximum Deformation. Firstly, it was found that a combination of 75% fill density, Z-axis orientation, and 0.4 mm layer height exhibits the best mechanical properties with their effectiveness in descending order, regardless of the printing velocity. Although:

1. The most effective printing parameters are building orientation, fill density, and layer height in the descending order, but there were no significant interaction between them.
2. Regarding to the obtained p-value, printing velocity has no critical influence on the responses.
3. The achieved Young's modulus, yield strength, and maximum strength of the injection molded parts were higher than printed ones taking into account the solidity percentages of the samples. Maximum deformation of the printed samples was considerably higher than injected samples.
4. Altogether, the achieved values for the responses of this material are not high enough as a thermoplastic composite which the composition percentage of the fibers to matrix could be one reason of its deficiency.

Author Contributions: Conceptualization, J.A.T.-R., J.J.-P. and R.J.-M.; Methodology, R.J.-M., M.D.Z. and J.L..; Software, J.L. and M.D.Z.; Validation, J.L., and R.J.-M.; Formal Analysis, J.A.T.-R., J.J.-P. and R.J.-M.; Investigation, J.A.T.-R., and M.D.Z.; Resources, J.A.T.-R. and J.L.; Data Curation, J.L., J.J.-P. and R.J.-M.; Writing-Original Draft Preparation, M.D.Z.; Writing-Review & Editing, J.L., J.A.T.-R. and R.J.-M.; Visualization, J.L. and R.J-.M.; Supervision, J.A.T.-R. and R.J.-M.; Project Administration, J.A.T.-R., Funding Acquisition, J.A.T.-R., R.J.-M. and J.L.

Funding: This research did not receive any specific grant from funding agencies in the public, commercial, or not-for-profit sectors.

Conflicts of Interest: The authors declare no conflict of interest.

Abbreviations

AM - additive manufacturing

FFF - fused filament fabrication

PLA - polylactic acid

DOE - design of experiments

ANOVA - analysis of variance

E - Young's modulus

$Rp_{0,2}$ - yield strength

σ_{max} - maximum strength

ε - maximum deformation

References

1. Jerez-Mesa, R.; Travieso-Rodriguez, J. A.; Llumà-Fuentes, J.; Gomez-Gras, G.; Puig, D. Fatigue lifespan study of PLA parts obtained by additive manufacturing. Procedia Manufacturing. **2017**, 13, 872-879.
2. Domingo-Espin, M.; Travieso-Rodriguez, J. A.; Jerez-Mesa, R.; Lluma-Fuentes, J. Fatigue performance of ABS specimens obtained by fused filament fabrication. Materials. **2018**, 11(12), 2521.
3. Fayazbakhsh, K.; Movahedi, M.; Kalman, J. The impact of defects on tensile properties of 3D printed parts manufactured by fused filament fabrication. Materials Today Communications. **2019**, 18, 140-148.
4. Morales-Planas, S.; Minguella-Canela, J.; Lluma-Fuentes, J.; Travieso-Rodriguez, J. A.; García-Granada, A. A. Multi Jet Fusion PA12 manufacturing parameters for watertightness, strength and tolerances. Materials. **2018**, 11(8), 1472.
5. Es-Said, O. S.; Foyos, J.; Noorani, R.; Mel Mendelson, Marloth, R.; Pregger, B. A. Effect of layer orientation on mechanical properties of rapid prototyped samples. Materials and Manufacturing Processes 15. **2000**, 1, 107-122.
6. Sood, A. K.; Ohdar, R. K.; & Mahapatra, S. S. Parametric appraisal of mechanical property of fused deposition modelling processed parts. Materials & Design. **2010**, 31(1), 287-295.
7. Fernandez-Vicente, M.; Calle, W.; Ferrandiz, S.; Conejero, A. Effect of infill parameters on tensile mechanical behavior in desktop 3D printing. 3D printing and additive manufacturing. **2006**, 3(3), 183-192.
8. Laureto, J. J.; Pearce, J. M. Anisotropic mechanical property variance between ASTM D638-14 type i and type iv fused filament fabricated specimens. Polymer Testing. **2018**, 68, 294-301.
9. Cwikla, G.; Grabowik, C.; Kalinowski, K.; Paprocka, I.; Ociepka, P. The influence of printing parameters on selected mechanical properties of FDM/FFF 3D-printed parts. In Materials Science and Engineering Conference Series. **2017**, 227, No. 1, 012033.
10. Marat-Mendes.; Rosa, M.; Guedes, M.; Leite, Baptista, R. Effect of Fused Filament Fabrication Processing Parameters on The Mechanical Properties of PLA Components. In XVI Portuguese Conference on Fracture. **2018**.
11. El Magri, A.; El Mabrouk, K.; Vaudreuil, S.; Ebn Touhami, M. Mechanical properties of CF-reinforced PLA parts manufactured by fused deposition modeling. Journal of Thermoplastic Composite Materials. **2019**, 0892705719847244.
12. Ozcelik, B.; Ozbay, A.; Demirbas, E. Influence of injection parameters and mold materials on mechanical properties of ABS in plastic injection molding. International Communications in Heat and Mass Transfer. **2010**, 37(9), 1359-1365.
13. Casavola, C.; Cazzato, A.; Moramarco, V.; Pappalettere, C. Orthotropic mechanical properties of fused deposition modelling parts described by classical laminate theory. Materials & design. **2016**, 90, 453-458.

14. Quintana, R.; Choi, J. W.; Puebla, K.; Wicker, R. Effects of build orientation on tensile strength for stereolithography-manufactured ASTM D-638 type I specimens. The International Journal of Advanced Manufacturing Technology. **2010**, 46(1-4), 201-215.
15. Galantucci, L. M.; Lavecchia, F.; Percoco, G. Quantitative analysis of a chemical treatment to reduce roughness of parts fabricated using fused deposition modeling. CIRP annals. 2010, 59(1), 247-250.
16. Maidin, S.; Mohamed, A. S.; Akmal, S.; Mohamed, S. B.; Wong, J. H. U. Feasibility study of vacuum technology integrated fused deposition modeling to reduce staircase effect. Journal of Fundamental and Applied Sciences. **2018**, 10(1S), 633-645.
17. Lederle, F.; Meyer, F.; Brunotte, G. P.; Kaldun, C.; Hübner, E. G. Improved mechanical properties of 3D-printed parts by fused deposition modeling processed under the exclusion of oxygen. Progress in Additive Manufacturing. **2016**, 1(1-2), 3-7.
18. Malinauskas, M.; Rekštytė, S.; Lukoševičius, L.; Butkus, S.; Balčiūnas, E.; Pečiukaitytė, M.; Baltriukienė, D.; Bukelskienė, V.; Butkevičius, A.; Kucevičius, P.; Rutkūnas, V. 3D microporous scaffolds manufactured via combination of fused filament fabrication and direct laser writing ablation. Micromachines. **2014**, 5(4), pp.839-858.
19. Nourbakhsh, A.; Ashori, A. Wood plastic composites from agro-waste materials: Analysis of mechanical properties. Bioresource technology. **2010**, 101(7), 2525-2528.
20. Tufan, M.; Güleç, T.; Peşman, E.; Ayrilmis, N. Technological and thermal properties of thermoplastic composites filled with heat-treated alder wood. BioResources. **2016**, 11(2), 3153-3164.
21. Tymrak, B. M.; Kreiger, M.; Pearce, J. M. Mechanical properties of components fabricated with open-source 3-D printers under realistic environmental conditions. Materials & Design. **2014**, 58, 242-246.
22. Mohamed, O. A.; Masood, S. H.; Bhowmik, J. L. Optimization of fused deposition modeling process parameters: a review of current research and future prospects. Advances in Manufacturing. **2015**, 3(1), 42-53.
23. Travieso-Rodriguez, J. A.; Jerez-Mesa, R.; Llumà, J.; Traver-Ramos, O.; Gomez-Gras, G.; Roa Rovira, J. J. Mechanical properties of 3D-printing Polylactic acid parts subjected to bending stress and fatigue testing. Materials. **2019**, 12(23), 3859.
24. Shabat, D.; Rosenthal, Y.; Ashkenazi, D.; Stern, A. Mechanical and structural characteristics of fused deposition modeling ABS material. Annals of “Dunarea de Jos” University, Fascicle XII, Welding Equipment and Technology. **2017**, 28, 16-24.